Chaos in random recurrent neural networks – *preliminary*

Tuan Pham

1. Overall description

The goal of my project is to quantitatively describe the stability of random neural networks, via replicating the main results of stability in recurrent neural networks with random connectivity in [1]. The stability of the network depends on the gain parameters of the nonlinear activation function of the artificial units.

Disclaimer: I am struggling to understand the mean-field theory derivation from [1] so I am trying a few things not following the text strictly, meaning the following derivations might not be rigorous, or possibly not correct. I based those modifications on a few sources, mainly [2, 3, 4]. [1]

2. Concept introduction

2.1. Single unit construction and activation

A biological neuron could be modelled by many different ways, from simple binary-switching units to detailed compartmental conductance-based models. For the sake of simplicity, a neuron input-output response could be modelled with a hyperbolic tangent (Equation 1) to scale the input from $(-\infty, \infty)$ monotonically to a bounded range between $[-1, 1]$.

$$\phi(x) = \tanh(gx + b) \tag{1}$$

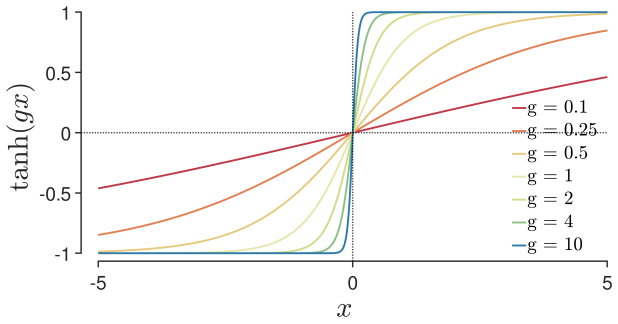

Figure 1: *Example of* $\tanh(gx)$ *for different gains*

The rationale is that small inputs would result in inactive state (nearer to -1) whereas larger inputs would lead to more active state (nearer to 1). The continuous range, when scaled from $[-1, 1]$ to $[0, 1]$, could be interpreted in many ways, for example the probability of spiking in a given time step, or a normalized firing rate. Additionally, the continuous range and smoothness are easier to work with than applying conditions for spiking like binary-switching models.

As for the parameters of the activation function, the gain g could be interpreted as the neuron's input resistance, whereas the bias b could be analogous to the opposite of a threshold for spiking or activated. Higher gain and larger bias would be appropriate to mimic the activation of a highly excitable neuron. For the sake of simplicity, I will ignore the bias terms for now ($b = 0$) and will integrate in the analysis later on if time permits. Examples of the activation functions for different gain parameters are shown in Figure 1. It will be shown later on that the activation gain parameter could be combined with a synaptic variance parameter to reduce the parameter dimension for analysis.

TODO: Integrate bias terms in if time allows.

2.2. Recurrent neural network

Assume we have N neurons, each with its continuous local field input h_i and their activated state $S_i = \phi(h_i)$, with $i = \overline{1, N}$. A recurrent network connects the presynaptic neuron j (source) with postsynaptic neuron i (target) with a weight (synaptic efficay) of $\mathbf{J}_{ij}$, so that the input from $j \to i$ is $\mathbf{J}_{ij} S_j$. For simplicity, we will only have 2 constraints on the weight matrix: (1) no self-connectivity, meaning $\mathbf{J}_{ii} = 0 \ \forall i$; and (2) $\mathbf{J}_{ij} \sim \mathcal{N}\left(0, J^2/N\right)$, independently from each other. It should be noted that this is overly simplified - as in biological neural networks, there are other important constraints on excitatory and inhibitory connectivity to be the least, and proportions of excitatory and inhibtory neurons, as well as synaptic dynamics.

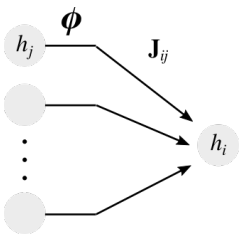

Figure 2: *Inputs to each unit of a recurrent network*

The governing equations for the local field variables are the system of the following Equation 2 (illustrated in Figure 2), without considering external outputs. The first term is analogous to a resting "leaky" term, whereas the latter corresponds to the weighted-sum of the inputs from presynaptic neurons.

[1] All of these are quite old papers, but seem quite important as they are highly cited.

$$\dot{h_i} = -h_i(t) + \sum_{j=1}^{N} \mathbf{J}_{ij} S_j = -h_i(t) + \sum_{j=1}^{N} \mathbf{J}_{ij} \phi(h_j) \tag{2}$$

3. Properties

3.1. Reduction of gain parameters $gJ \leftarrow g$

Although in [1], the parameters of investigation include both the nonlinear gain g and the variability of the synaptic weights J, more specifically the product gJ. However, we could easily reduce such product to just one variable g and set $J = 1$. More specifically, divide Equation 2 by J, we'd have:

$$\frac{d(h_i/J)}{dt} = \frac{h_i}{J} + \sum_{j=1}^{N} \frac{\mathbf{J}_{ij}}{J} \tanh\left[(gJ) \times \frac{h_j}{J}\right] \tag{3}$$

Because $\mathbf{J}_{ij} \sim \mathcal{N}\left(0, J^2/N\right) \implies \mathbf{J}_{ij}/J \sim \mathcal{N}\left(0, 1/N\right)$. Now, we can make the following substitutions to Equation 3 to have Equation 2 with just one parameter g:

$$\begin{cases} gJ & \leftarrow g \\ h_i/J & \leftarrow h_i \\ \mathbf{J}_{ij}/J & \leftarrow \mathbf{J}_{ij} \sim \mathcal{N}\left(0, 1/N\right) \end{cases}$$

3.2. Jacobian

The derivative of the activation function with respect to the local field variable is

$$\phi'(x) = \frac{\partial \phi}{\partial x} = g\left(1 - \tanh^2(x)\right) = g\left(1 - \phi^2(x)\right)$$

Hence, the Jacobian of system could be expressed as Equation 4, with $\overrightarrow{h}$ as a column vector of the local field variables, and the element-wise multiplication operator $\circ$ defined as followed for a matrix $\mathbf{J}$ and a row vector $\overrightarrow{h}^T$: $\left[\mathbf{J} \circ \overrightarrow{h}^T\right]_{ij} = \mathbf{J}_{ij} \cdot h_j$.

$$Df = g\mathbf{J} \circ \left(1 - \phi^2\left[\overrightarrow{h}^T\right]\right) - \mathbf{I} \tag{4}$$

The explicit expression is useful for numerical calculation of the maximal Lyapunov exponent, as in [5], and implimented in MATLAB on [6].

TODO: Summarize Lyapunov calculation implementation either in [5] or [7]

4. Stability analysis

4.1. Stability analysis in discrete time

Although the problem is set in continuous time as originally in [1], it seems that it is easier to analyze in discrete time (like in [2]). Hence I will be analyzing the stability of the system in discrete time ($dt = 1$), then show simulation results of the continuous version (small dt). With $dt = 1$, $\dot{h} = h(t+1) - h(t)$, then Equation 2 becomes:

$$h_i(t+1) = \sum_{j=1}^{N} \mathbf{J}_{ij} \phi(h_j) \tag{5}$$

Local chaos hypothesis: To summarize from [3, 4], as $N \to \infty$, without the constraints of symmetric coupling (as in $\mathbf{J}_{ij} \neq \mathbf{J}_{ji}$), the local field variables $h_i(t)$ can be treated as independent from each other, and from the random weights in $\mathbf{J}$. In this case, they would be independent Gaussian processes. And we would just need to focus on one variable in the thermodynamic limit.

Because there are no bias terms and $\langle \mathbf{J} \rangle = 0$, we would expect $\langle h(t) \rangle = 0$, as in zero-mean. So now we'd focus on the second moment, which is also the variance (because mean is 0), of the local field variable: $\nu(t) = \langle h^2(t) \rangle$.

$$h_i \sim \mathcal{N}(0, \nu(t)) \tag{6}$$

Additionally, we also define $q(t) = \langle \phi^2(h(t)) \rangle = \text{var}(\phi(h(t))$ (because mean is also 0). Let's call x as a random variable with normally distributed with unit variance zero mean, $x \sim \mathcal{N}(0, 1)$ and $p_{\mathcal{N}}(x) = \frac{1}{\sqrt{2\pi}} \exp\left(-\frac{1}{2}x^2\right)$. Because of Equation 6 and $x\sqrt{\nu(t)} \sim \mathcal{N}(0, \nu(t))$, we can rewrite $q(t)$ as following:

$$q(t) = \int_{-\infty}^{\infty} \phi^2\left(x\sqrt{\nu(t)}\right) p_{\mathcal{N}}(x) dx \tag{7}$$

Because h_i and $\mathbf{J}_{ij}$ are independent and that their means are 0, we'd have $\text{var}(\mathbf{J}_{ij}\phi(h_j)) = \text{var}(\mathbf{J}_{ij})q(t) = q(t)/N$. Combined with Equation 5 and Equation 7:

$$\nu(t+1) = \langle h^2(t+1) \rangle = N \times \frac{1}{N} q(t) = q(t) = \int_{-\infty}^{\infty} \phi^2\left(x\sqrt{\nu(t)}\right) p_{\mathcal{N}}(x) dx \tag{8}$$

Let's call $\mathcal{M}(\nu(t))$ as the left-hand side of Equation 8. Then we have a 1-D discrete mapping $\nu(t+1) = \mathcal{M}(\nu(t))$ and we could attempt to investigate the existence of a fixed point ν^* as $t \to \infty$. The fixed point would satisfy $\nu^* = \mathcal{M}(\nu^*)$. We could make assumption about the fixed point and do a Taylor expansion to reach an analytic approximation. However, the actual values of ν^* are less important, so we could evaluate it graphically for ease (Figure 3, left).

Additionally, as shown in [2], the maximum Lyapunov exponent could be expressed as function of the fixed point, as followed:

$$\lambda = \frac{1}{2} \log \int_{-\infty}^{\infty} \left[\phi'\left(\sqrt{\nu^*}x\right)\right]^2 p_{\mathcal{N}}(x) dx \tag{9}$$

TODO: Prove Equation 9

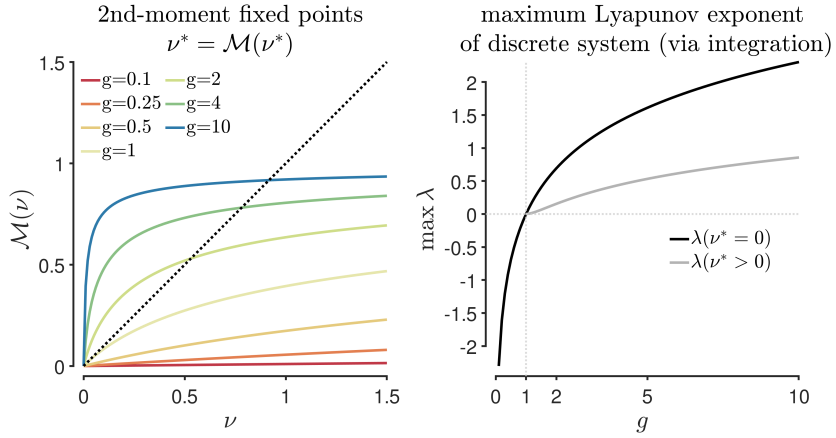

Figure 3: *Analysis of second moment fixed points and the corresponding maximal Lyapunov exponent of the discrete version.* (**Left**) Second moment fixed points following Equation 8 for different gains g (colors). The fixed points are at the intersection of the identity line and the colored curves. (**Right**) The maximum Lyapunov exponent as obtained via integration in Equation 9, as a function the nonlinear gain g. The black line corresponds to $\nu^* = 0$, whereas the gray line corresponds to $\nu^* > 0$ (only for $g > 1$).

As illustrated in Figure 3 (left), it can be seen that for $g \leq 1$, there is only one fixed point, which is $\nu^* = 0$, which is actually stable as the maximal Lyapunov exponent calculated via Equation 9 are negative (Figure 3, right). However, for $g > 1$, aside from $\nu^* = 0$ as a fixed point, there is another nonzero fixed point within the unit

square. Both of the maximal Lyapunov exponents corresponding to these 2 fixed points for each g are positive, indicating chaotic regime.

UNCERTAIN: whether the actual magnitudes of Lyapunov exponents between discrete time and continuous time system agree

4.2. Simulations of continuous system

I ran continuous time (as in $dt < 1$) simulation for $N = 200$ until $t = 100$. For each value of g, I had 10 realizations of the network ($\mathbf{J} \sim \mathcal{N}(0, 1)$) and initial conditions h_0. I used the implemented package from [6] to calculate the Lyapunov exponent. The results are shown in Figure 4.

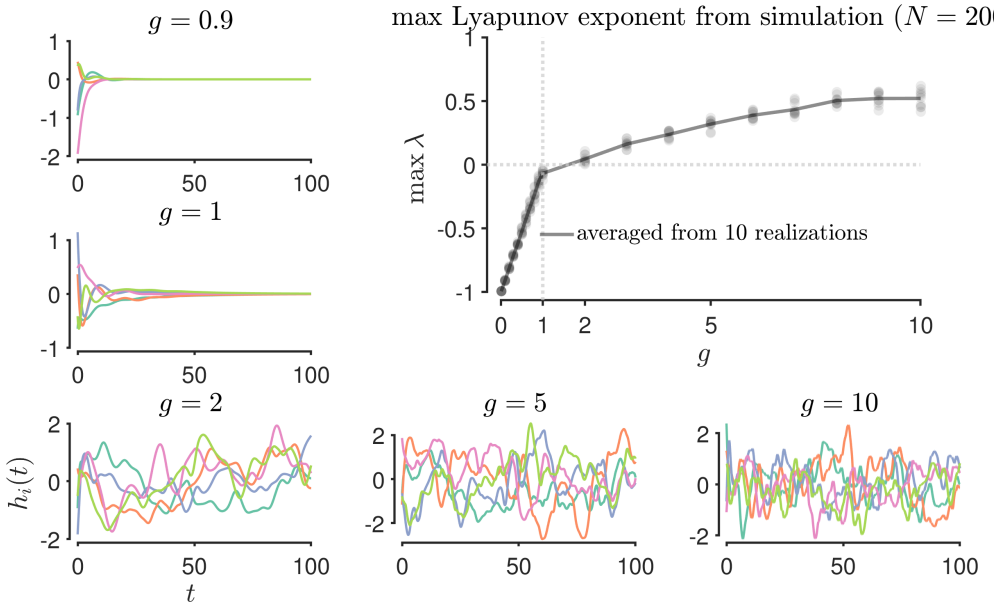

Figure 4: *Lyapunov exponents of the continuous timed simulations.* The small panels on the left and bottom show examples of the simulations for different values of g. Plotted are 5 randomly chosen local field variables $h_i(t)$ in 200 neurons. The top right panel shows the maximal Lyapunov exponents at the end of the simulation ($t = 100$) estimated via [6], averaged across 10 different realizations of the weight matrix and initial conditions.

First of all, as expected, for $g \leq 1$, the solutions seem to decay to $h_i = 0$. This agrees with $\nu^* = 0$, as discussed above. The sign of the maximal Lyapunov exponents also seem to agree generally with the discrete case (Figure 3, right). This supports that this fixed point is stable.

Secondly, for many of $g > 1$, the activity of the network tends towards chaotic in the simulations, as also supported by the positivity of the maximal Lyapunov exponents (Figure 4, right). This, in the gross part, agrees with the positivity observed in the discrete case (Figure 3).

Disregarding the mismatch between actual magnitudes between the discrete and continuous versions, the signs, which in turn indicate the stability of the system, do seem to agree, with the exception of g near 1, particularly the range of $1 < g < 2$. There might be more points in this range that could correspond to negative λ. Additionally, this could be due to the possibility that N is not large enough.

TODO: Rerun simulations for longer with larger N, finer scale between of $g \in [0.9, 2]$

TODO: Inspect where limit cycles arise, and further investigate period doubling

Notes

References

[1] H. Sompolinsky, A. Crisanti, and H. J. Sommers. Chaos in random neural networks. *Phys. Rev. Lett.*, 61:259–262, Jul 1988.

[2] L. Molgedey, J. Schuchhardt, and H. G. Schuster. Suppressing chaos in neural networks by noise. *Physical Review Letters*, 69(26):3717–3719, December 1992.

[3] B. Cessac. Increase in Complexity in Random Neural Networks. *Journal de Physique I*, 5(3):409–432, March 1995.

[4] B. Doyon, B. Cessac, M. Quoy, and M. Samuelides. Mean-field equations, bifurcation map and chaos in discrete time, continuous state, random neural networks. *Acta Biotheoretica*, 43(1-2):169–175, June 1995.

[5] Alan Wolf, Jack B. Swift, Harry L. Swinney, and John A. Vastano. Determining lyapunov exponents from a time series. *Physica D: Nonlinear Phenomena*, 16(3):285 – 317, 1985.

[6] Vasiliy Govorukhin. *Calculation Lyapunov Exponents for ODE*, Retrieved May 19, 2020. MATLAB Central File Exchange.

[7] Hubertus F. [von Bremen], Firdaus E. Udwadia, and Wlodek Proskurowski. An efficient qr based method for the computation of lyapunov exponents. *Physica D: Nonlinear Phenomena*, 101(1):1 – 16, 1997.